Steady-State Density Functional Theory for Finite Bias Conductances

G. Stefanucci[1, 2] and S. Kurth[3, 4]

[1]*Dipartimento di Fisica, Università di Roma Tor Vergata and European Theoretical Spectroscopy Facility (ETSF),*
Via della Ricerca Scientifica 1, 00133 Rome, Italy
[2]*INFN, Laboratori Nazionali di Frascati, Via E. Fermi 40, 00044 Frascati, Italy*
[3]*Nano-Bio Spectroscopy Group and European Theoretical Spectroscopy Facility (ETSF),*
Dpto. de Física de Materiales, Universidad del País Vasco UPV/EHU, Av. Tolosa 72, E-20018 San Sebastián, Spain
[4]*IKERBASQUE, Basque Foundation for Science, Maria Diaz de Haro 3, E-48013 Bilbao, Spain*

In the framework of density functional theory a formalism to describe electronic transport in the steady state is proposed which uses the density on the junction and the *steady current* as basic variables. We prove that, in a finite window around zero bias, there is a one-to-one map between the basic variables and both local potential on as well as bias across the junction. The resulting Kohn-Sham system features two exchange-correlation (xc) potentials, a local xc potential and an xc contribution to the bias. For weakly coupled junctions the xc potentials exhibit steps in the density-current plane which are shown to be crucial to describe the Coulomb blockade diamonds. At small currents these steps emerge as the equilibrium xc discontinuity bifurcates. The formalism is applied to a model benzene junction, finding perfect agreement with the orthodox theory of Coulomb blockade.

Engineering electrical transport through molecular junctions is a mandatory passage toward the miniaturization and speeding up of device components [1, 2]. As a systematic experimental characterization of every synthesizable molecule is impractical, reliable theoretical methods are of utmost importance to progress. Density Functional Theory (DFT) has emerged as the method of choice due to the chemical complexity of the junctions [3–7]. Nevertheless, to date there exists still no DFT scheme to deal with the ubiquitous Coulomb Blockade (CB) phenomenon. CB stems from the interplay between quantum confinement and Coulomb repulsion, and it leaves clear fingerprints in the measured conductances.

As recognized by several authors [8–12], the discontinuity of the exchange-correlation (xc) potential plays a pivotal role in blocking the electron density at integer values. Although at low temperatures and for single-channel junctions this key xc feature yields also accurate DFT conductances [13–18], we showed that at finite temperature and/or bias the *exact* DFT conductance does not exhibit any CB signature [11]. In fact, static DFT misses the dynamical xc bias corrections [19–22] predicted by Time-Dependent (TD) DFT [23], the proper framework within which to formulate a theory of quantum transport [19, 20]. Only recently a dynamical xc correction has been proposed [11], but its applicability is limited to the CB regime at zero bias.

In this Letter we put forward a steady-state DFT, henceforth named i-DFT, whose xc potentials (gate and bias) are functionals of the molecular density and the *steady-state* current. The i-DFT framework is suited to study the finite-bias and finite-temperature conductance as function of external gate and applied bias, and it generalizes standard DFT in equilibrium. Unlike Current DFT [24] (CDFT), i-DFT applies out of equilibrium
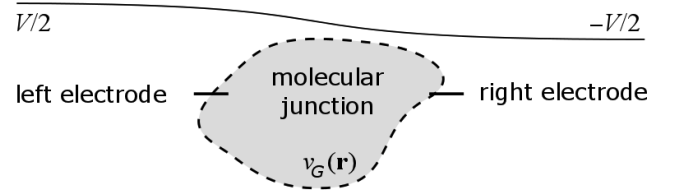

FIG. 1. Schematic illustration of a molecular junction attached to a left and right electrode. The system is subject to a bias voltage V (solid line) and a gate potential $v_G(\mathbf{r})$. The grey area is the molecular region defined in the main text.

and unlike TD(C)DFT [25, 26] the i-DFT functional has no memory. The empirical Landauer+DFT approach to transport [3–7] is recovered as an approximation to i-DFT with the xc bias set to zero. As we shall see this approximation is too severe in the CB regime.

Through a reverse-engineering procedure we show that the well-known discontinuities of the DFT xc potential at integer particle number N *bifurcate* as the current I starts flowing. The xc gate and xc bias exhibit an intricate and, at first sight, inexplicable pattern of intersecting steps in the N-I plane. We recognize, however, that every intersection occurs at the plateau values of N and I in a CB diamond. This "duality" between intersections and CB plateaus in current and particle number is an exact property of the xc potentials of nonequilibrium open systems and the fundamental ingredient to extend DFT transport calculations to finite bias.

i-DFT We consider a current-carrying molecular junction attached to a left (L) and right (R) electrode in the *steady state*, see Fig. 1. In addition to the nuclear potential $v_n(\mathbf{r})$ the electrons are subject to an external bias $v_B(\mathbf{r})$ generated by a battery and to an external gate

$v_G(\mathbf{r})$ that vanishes deep inside the electrodes. The classical potential $v_n(\mathbf{r}) + v_B(\mathbf{r}) + v_H(\mathbf{r})$, v_H being the Hartree potential, in the far L (R) region differs by a uniform shift $V/2$ ($-V/2$) from its equilibrium value, V being the applied bias.[27] Since a change of the external gate does not affect the value of V we can unambiguously calculate the steady-state current and density by specifying $v_n(\mathbf{r})$, $v_G(\mathbf{r})$ and V. [19, 20]

Let us select an arbitrary *finite* region of space $\mathcal{R}$ around the molecule, henceforth named *molecular region*, and write the nuclear/gate potential as $v_{n/G}(\mathbf{r}) = v_{n/G}^{\rm in}(\mathbf{r}) + v_{n/G}^{\rm out}(\mathbf{r})$ where $v_{n/G}^{\rm in}(\mathbf{r}) = v_{n/G}(\mathbf{r})$ for $\mathbf{r} \in \mathcal{R}$ and zero otherwise. Similarly, we write the electronic density as $n(\mathbf{r}) = n^{\rm in}(\mathbf{r}) + n^{\rm out}(\mathbf{r})$ where $n^{\rm in}(\mathbf{r}) = n(\mathbf{r})$ for $\mathbf{r} \in \mathcal{R}$ and zero otherwise. We advance that for practical applications a convenient choice of the molecular region is the one for which in the electrodes (outside $\mathcal{R}$) we have $v_G \simeq 0$ and $v_n + v_H$ weakly dependent on the chemical structure of the junction. In this case $n^{\rm out}(\mathbf{r})$ is not affected by a change in v_G, a condition used in all DFT-based quantum transport calculations. However, the formal results contained in this section are independent of the choice of $\mathcal{R}$.

The foundation of i-DFT rests on the one-to-one correspondence between the two pairs $(v^{\rm in}(\mathbf{r}), V)$ and $(n^{\rm in}(\mathbf{r}), I)$. The first pair consists of the molecular potential $v^{\rm in}(\mathbf{r}) \equiv v_n^{\rm in}(\mathbf{r}) + v_G^{\rm in}(\mathbf{r})$ and the bias V whereas the second pair consists of the molecular density $n^{\rm in}(\mathbf{r})$ and the steady current I.

Theorem.– For any *finite* temperature and at *fixed* outer potential $v^{\rm out}(\mathbf{r}) \equiv v_G^{\rm out}(\mathbf{r}) + v_n^{\rm out}(\mathbf{r})$ the map $(v^{\rm in}(\mathbf{r}), V) \rightarrow (n^{\rm in}(\mathbf{r}), I)$ is invertible in a finite bias window around $V = 0$.

Proof.– To prove the theorem we show that the Jacobian

$$J_{V=0} = {\rm Det} \begin{bmatrix} \delta n^{\rm in}(\mathbf{r})/\delta v^{\rm in}(\mathbf{r}') & \partial n^{\rm in}(\mathbf{r})/\partial V \\ \delta I/\delta v^{\rm in}(\mathbf{r}') & \partial I/\partial V \end{bmatrix}_{V=0}. \quad (1)$$

is nonvanishing (we are of course working under the physically reasonable assumption that $n^{\rm in}(\mathbf{r})$ and I are continuously differentiable, which also implies that J_V is continuous in $V = 0$). The block $\chi^{\rm in}(\mathbf{r}, \mathbf{r}') \equiv \delta n^{\rm in}(\mathbf{r})/\delta v^{\rm in}(\mathbf{r}')|_{V=0}$ is the static *equilibrium* density response function of the contacted system with $\mathbf{r}, \mathbf{r}'$ in the molecular region, whereas $G \equiv \partial I/\partial V|_{V=0}$ is the zero-bias conductance. We start by showing that $\chi^{\rm in}$ is invertible for any molecular region $\mathcal{R}$. The equilibrium response function $\chi^{\rm in}$ can be calculated using leads of finite length L and then taking the limit $L \rightarrow \infty$. Let $\{|\Psi_i\rangle\}$ be a complete set of many-body eigenstates of the equilibrium *contacted* system with energy E_i and number of particles N_i. At temperature $1/\beta$ and chemical potential

μ the Lehmann representation of $\chi^{\rm in}$ reads [28]

$$\chi^{\rm in}(\mathbf{r}, \mathbf{r}') = \frac{1}{Z} \sum_{ij} \frac{f_{ij}(\mathbf{r}) f_{ij}(\mathbf{r}')}{\Omega_{ij}^2 + \eta^2} \Omega_{ij} \left(e^{-\beta E_i} - e^{-\beta E_j}\right) e^{\beta \mu N_i} \quad (2)$$

with Z the partition function, $\Omega_{ij} = E_i - E_j$ the energy difference, η a positive infinitesimal to set to zero after the limit $L \rightarrow \infty$, and $f_{ij}(\mathbf{r}) = \langle \Psi_i | \hat{n}(\mathbf{r}) | \Psi_j \rangle - \delta_{ij} n(\mathbf{r})$ the excitation amplitudes. We define $T_{ij} \equiv \int_\mathcal{R} d\mathbf{r} f_{ij}(\mathbf{r}) t(\mathbf{r})$ where $t(\mathbf{r})$ is a test function. Notice that T_{ij} has a well defined limit for $L \rightarrow \infty$ since the integral is over the finite domain $\mathcal{R}$. Proving the invertibility of $\chi^{\rm in}$ is equivalent to proving that

$$\int_\mathcal{R} d\mathbf{r} d\mathbf{r}' t(\mathbf{r}) \chi^{\rm in}(\mathbf{r}, \mathbf{r}') t(\mathbf{r}') = \frac{1}{Z} \sum_{ij} \frac{|T_{ij}|^2}{\Omega_{ij}^2 + \eta^2} \Omega_{ij}$$
$$\times \left(e^{-\beta E_i} - e^{-\beta E_j}\right) e^{\beta \mu N_i} \neq 0 \quad (3)$$

for any test function $t(\mathbf{r})$. To this end we observe that for every $E_i \lessgtr E_j$ we have $\Omega_{ij} \lessgtr 0$ and $\left(e^{-\beta E_i} - e^{-\beta E_j}\right) \gtrless 0$. Hence the left hand side of Eq. (3) is non-positive and can be zero only provided that $T_{ij} = 0$ for every $E_i \neq E_j$. However, this latter circumstance implies that the Hamiltonian and the operator $\hat{T} \equiv \int_\mathcal{R} d\mathbf{r} \, \hat{n}(\mathbf{r}) t(\mathbf{r})$ can be diagonalized simultaneously, an absurdum for any test function $t(\mathbf{r})$. Therefore Eq. (3) holds true and $\chi^{\rm in}$ is invertible. Similarly, from the Lehmann representation of the zero-bias conductance [29]

$$G = -\frac{1}{Z} \sum_{ij} \frac{2\eta |I_{ij}|^2}{(\Omega_{ij}^2 + \eta^2)^2} \Omega_{ij} \left(e^{-\beta E_i} - e^{-\beta E_j}\right) e^{\beta \mu N_i} \quad (4)$$

one finds the intuitive result $G > 0$. In Eq. (4) $I_{ij} \equiv \langle \Psi_i | \hat{I} | \Psi_j \rangle$ with $\hat{I}$ the longitudinal current operator. The crucial observation to end the proof is that at zero bias a variation of $v^{\rm in}$ does not induce a steady current, hence $\delta I/\delta v^{\rm in}(\mathbf{r}')|_{V=0} = 0$. We conclude that $J_0 = {\rm Det}[\chi^{\rm in}]G < 0$ for all $v^{\rm in}$. Since J_V is a continuous function of V around $V = 0$, there exists a finite interval (depending on $v^{\rm in}$) around $V = 0$ for which $J_V < 0$. In this domain the map $(v^{\rm in}(\mathbf{r}), V) \rightarrow (n^{\rm in}(\mathbf{r}), I)$ is invertible.

An interesting consequence of the i-DFT theorem is that at zero bias (and hence at zero current) it generalizes standard equilibrium DFT at finite temperatures [30] to portions of an interacting system. In fact, the i-DFT theorem implies that two potentials v and v' differing only in a region $\mathcal{R}$ generate two equilibrium densities $n(\mathbf{r})$ and $n'(\mathbf{r})$ which are certainly different in $\mathcal{R}$ (see also Ref. 31). It is worth observing that the zero-bias i-DFT does not suffer from the DFT problem of infinite systems [32] since the map involves only the density and the potential in $\mathcal{R}$. Furthermore, since we are not interested in the density outside $\mathcal{R}$, no assumption on the analyticity of the density in position space is needed [33]. Interestingly, the zero-bias i-DFT for infinite systems can easily be generalized to the time domain too. Indeed, the boundary

term in the Runge-Gross proof [23] vanishes identically since $v - v'$ is, by definition, zero outside $\mathcal{R}$.

Henceforth we omit the superscript "in" in the molecular density and potential; thus $n(\mathbf{r})$ and $v(\mathbf{r})$ are always calculated in $\mathbf{r} \in \mathcal{R}$. Let (n, I) be the molecular density and current induced by the potentials (v, V) in an *interacting* junction. Under the usual assumption of noninteracting v-representability, the i-DFT theorem guarantees that a pair of potentials (v_s, V_s) which reproduces the same (n, I) in a *noninteracting* junction is unique. Following the Kohn-Sham (KS) procedure we define the xc bias and Hartree-xc (Hxc) gate as

$$V_{\mathrm{xc}}[n, I] \equiv V_s[n, I] - V[n, I], \tag{5a}$$

$$v_{\mathrm{Hxc}}[n, I](\mathbf{r}) \equiv v_s[n, I](\mathbf{r}) - v[n, I](\mathbf{r}). \tag{5b}$$

The nomenclature Hxc gate instead of Hxc molecular potential is used for brevity to indicate that v_{Hxc} is nonzero only in the molecular region. The self-consistent KS equations then read (hereafter $\int \equiv \int \frac{d\omega}{2\pi}$)

$$n(\mathbf{r}) = 2 \sum_{\alpha=L,R} \int f\left(\omega + s_\alpha \frac{V + V_{\mathrm{xc}}}{2}\right) A_\alpha(\mathbf{r}, \omega), \tag{6a}$$

$$I = 2 \sum_{\alpha=L,R} \int f\left(\omega + s_\alpha \frac{V + V_{\mathrm{xc}}}{2}\right) s_\alpha T(\omega). \tag{6b}$$

In Eqs. (6), $f(\omega) = 1/(e^{\beta(\omega - \mu)} + 1)$ is the Fermi function whereas $s_{R/L} = \pm$. We also defined the partial spectral function $A_\alpha(\mathbf{r}, \omega) \equiv \langle \mathbf{r}|\mathcal{G}(\omega)\Gamma_\alpha(\omega)\mathcal{G}^\dagger(\omega)|\mathbf{r}\rangle$, with $\mathcal{G}$ and Γ_α the KS Green's function and broadening matrices [28], and the transmission function $T = \mathrm{Tr}\left[\mathcal{G}(\omega)\Gamma_L(\omega)\mathcal{G}^\dagger(\omega)\Gamma_R(\omega)\right]$. In Eqs. (6) one should note the presence of the KS bias $V_s = V + V_{\mathrm{xc}}$ instead of the bare bias V; this comes from the mapping $(n, I) \leftrightarrow (v_s, V_s)$. Although the KS Eqs. (6) for n and I are formally identical to the TDDFT expressions of Ref. 19, 20, we stress that the i-DFT xc potentials depend on the *steady-state* molecular density and current while the TDDFT xc potential depend on the full history of the molecular *and* lead densities. The augmented local character of the i-DFT xc potentials is in agreement with similar findings in TDCDFT [34, 35].

The simplifications brought about by i-DFT are especially evident when considering the zero-bias conductance. From Eq. (6b) we have

$$G = G_s \left[1 + \frac{\partial V_{\mathrm{xc}}}{\partial I} G + \int d\mathbf{r} \frac{\delta V_{\mathrm{xc}}}{\delta n(\mathbf{r})} \frac{\partial n(\mathbf{r})}{\partial V}\right]_{V=0}, \tag{7}$$

with $G_s \equiv -2 \int f'(\omega) T(\omega)$ the zero-bias KS conductance. Since $I = 0$ is the solution of the KS equations with $V = 0$ and since $V_{\mathrm{xc}}[n, 0] = 0$ (for otherwise there would be a current flowing in the system at zero bias, in contradiction to the theorem) we have

$\delta V_{\mathrm{xc}}[n, I]/\delta n(\mathbf{r})|_{V=0} = \delta V_{\mathrm{xc}}[n, 0]/\delta n(\mathbf{r}) = 0$. Therefore

$$G = \frac{G_s}{1 - G_s \frac{\partial V_{\mathrm{xc}}}{\partial I}\big|_{I=0}}. \tag{8}$$

The i-DFT correction to G_s is physically more transparent than the TDDFT correction involving the zero-momentum and zero-frequency limit of the xc kernel [11, 16, 21, 36].

Although i-DFT has been formulated in $\mathbf{r}$-space the same theorem and KS procedure apply to tight-binding models by replacing $\mathbf{r}$ with a site or orbital index. To highlight the distinctive features of the i-DFT potentials in the CB regime, hence above the Kondo temperature, we apply the formalism to a junction described by the Constant Interaction Model (CIM) with Hamiltonian $\hat{H} = \sum_{i\sigma} \varepsilon_i \hat{n}_{i\sigma} + \frac{1}{2}U \sum_{i\sigma \neq j\sigma'} \hat{n}_{i\sigma} \hat{n}_{j\sigma'}$, where $\hat{n}_{i\sigma}$ is the occupation operator of the i-th level with spin σ.[37, 38] As the electron-electron interaction is confined to the molecular junction the Hartree potential vanishes in the leads. If we choose the region $\mathcal{R}$ as the set of interacting levels then the i-DFT theorem states that there is a one-to-one map between the pair $(\{\varepsilon_i\}, V)$ and the pair $(\{n_i\}, I)$.

Anderson model The CIM with one level coupled to two featureless leads, $\Gamma_\alpha(\omega) = \gamma/2$, is equivalent to the Anderson model. Due to spin-degeneracy the i-DFT potentials depend on the particle number $N = n_{1\uparrow} + n_{1\downarrow}$ and current I. For $\varepsilon_1 = v$, these can be calculated from

$$N = \int [f(\omega - V/2) + f(\omega + V/2)] A(\omega - v) \tag{9a}$$

$$I = \frac{\gamma}{2} \int [f(\omega - V/2) - f(\omega + V/2)] A(\omega - v), \tag{9b}$$

with $A(\omega)$ the interacting spectral function. Above the Kondo temperature T_K a good approximation for the spectral function is $A(\omega) = \frac{N}{2}\ell(\omega - U) + (1 - \frac{N}{2})\ell(\omega)$ with $\ell(\omega) = \gamma/(\omega^2 + \gamma^2/4)$ [39]. We verified (not shown) that N and I are in excellent agreement with the results of the Rate Equations [37, 40] (RE), the orthodox theory of CB for weakly coupled systems. For the Anderson model the map $(v, V) \to (N, I)$ is invertible for all V (infinite bias window) since the finite-bias Jacobian is

$$J_V = -2\gamma \frac{a_+ a_-}{2 - b_+ - b_-} \tag{10}$$

where $a_\pm = \int f'(\omega \pm V/2) A(\omega - v)$ and $b_\pm = \int f(\omega)[\ell(\omega - v - U \mp V/2) - \ell(\omega - v \mp V/2)]$. As $a_\pm < 0$ and $-1 < b_\pm < 0$ we find $J_V < 0$ [41].

To find the xc potentials in Eqs. (5) we invert the map $(v, V) \to (N, I)$ of Eqs. (9) for $U \neq 0$ and for $U = 0$. In terms of the variables $w_\pm = v \pm V/2$ the problem is separable since the map reads $N \mp 2I/\gamma = 2 \int f(\omega) A(\omega - w_\pm) \equiv \mathfrak{n}(w_\pm)$, which we solve by the bisection method. The values of $\mathfrak{n} \in [0, 2]$ and therefore the domain spanned by the particle number and current is $|I| \leq \frac{\gamma}{2} N$ for $N \in$
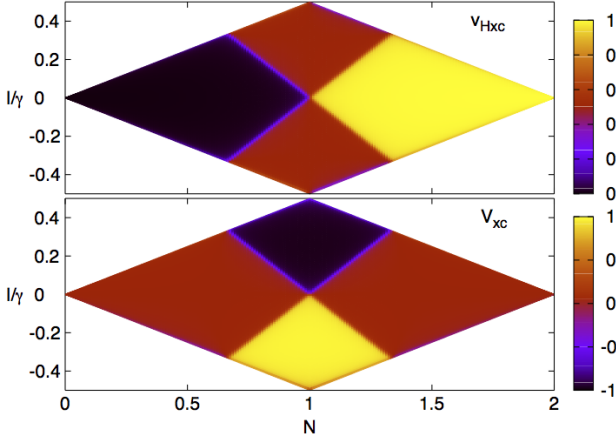
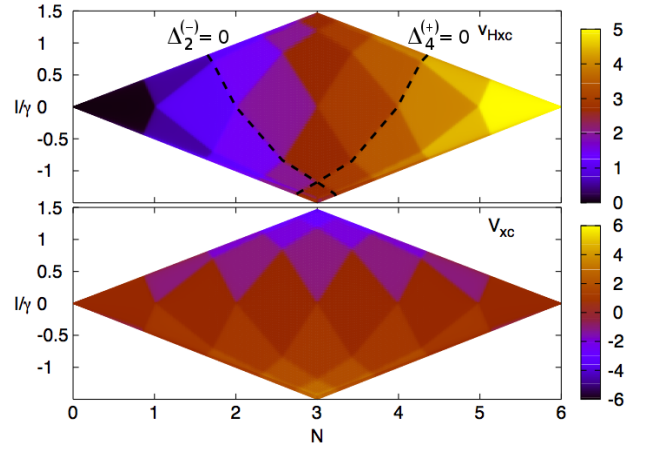FIG. 2. Hartree xc gate (top) and xc bias (bottom) of the Anderson model. Energies are in units of U.

FIG. 3. Hartree xc gate (top) and xc bias (bottom) of the three-degenerate level CIM. The edges of two steps with positive and negative slopes are highlighted with dashed lines. Energies are in units of U.

$[0, 1]$ and $|I| \leq \frac{\gamma}{2}(2 - N)$ for $N \in [1, 2]$. The reverse engineered xc potentials v_{Hxc} and V_{xc} are shown in Fig. 2 and three observations arise. (i) The Hxc gate (xc bias) exhibits smeared steps of height $U/2$ (U) along the lines $N = 1 \mp I/\gamma$. Interestingly, the DFT xc discontinuity of $v_{\mathrm{Hxc}}[N, 0]$ in $N = 1$ *bifurcates* as current starts flowing. (ii) The signs of V_{xc} and I are opposite (in agreement with the results of Ref. 42) and the derivative $\frac{\partial V_{\mathrm{xc}}}{\partial I}|_{I=0} < 0$, thus setting G_s as the upper limit for the interacting zero-bias conductance [see Eq. (8)]. In Ref. 11 we found that the zero-bias TDDFT correction at $N = 1$ can be expressed in terms of the Hxc gate as $\simeq 1/(\frac{2}{\gamma} G_s \frac{\partial v_{\mathrm{Hxc}}}{\partial N})$. A comparison with Eq. (8) suggests the existence of a relation (at least in the Anderson model) between V_{xc} and v_{Hxc} since for the two schemes to agree $\frac{\partial V_{\mathrm{xc}}}{\partial I}|_{I=0} = -\frac{2}{\gamma} \frac{\partial v_{\mathrm{Hxc}}}{\partial N}|_{I=0} \gg 1/G_s$. (iii) At finite bias $|V| < U$ and particle number $N = 1$ the CB prevents current flow in the interacting system. In the same situation the KS level pins to the chemical potential and I would be large if it were not for the counteraction of the xc bias $V_{\mathrm{xc}} = -V$. The Landauer+DFT approach [3–7] would therefore fail dramatically as it misses xc bias corrections.

We look for a parametrization of the xc potentials with the following properties: (*a*) at zero current $V_{\mathrm{xc}} = 0$ and v_{Hxc} reduces to the Hxc gate of Ref. 11 (*b*) occurrence of smeared steps of height $U/2$ for v_{Hxc} (and U for V_{xc}) at $N = 1 \mp I/\gamma$ and (*c*) the derivatives $\frac{\partial V_{\mathrm{xc}}}{\partial I}|_{I=0}$ and $\frac{\partial v_{\mathrm{xc}}}{\partial N}|_{I=0}$ are related as discussed in observation (iii). The xc potentials

$$v_{\mathrm{Hxc}}[N, I] = \frac{U}{4} \sum_{s=\pm} \left[1 + \frac{2}{\pi} \mathrm{atan} \frac{N + \frac{s}{\gamma}I - 1}{W} \right] \quad (11a)$$

$$V_{\mathrm{xc}}[N, I] = -U \sum_{s=\pm} \frac{s}{\pi} \mathrm{atan} \frac{N + \frac{s}{\gamma}I - 1}{W} \quad (11b)$$

have the required properties. If we choose the fitting

parameter $W \simeq 0.16 \gamma / U$, i-DFT with the xc potentials of Eqs. (11) produces self-consistent currents and densities which are almost indistinguishable from the interacting ones (not shown), including the density plateaus at $\frac{2}{3}$ and $\frac{4}{3}$ as well as the 2:1 ratio of the step heights in the current [43]. Remarkably, all this is achieved without breaking the spin symmetry.

Notice also that in Ref. 10 there was no xc bias and the current did not reach a steady-state value since the fitting parameter W was set to zero (in this case no self-consistent solution of the steady-state equation exists).

Multiple-level degenerate CIM Let us generalize the analysis to a CIM Hamiltonian with $\mathcal{M}$ degenerate levels $\varepsilon_i = v$ coupled to featureless leads, $\Gamma_{\alpha,ij}(\omega) = \delta_{ij}\gamma/2$. Due to degeneracy v_{Hxc} is uniform and depends only on $N = \sum_{i\sigma} n_{i\sigma}$ and I. Above T_K the particle number and current of the interacting and noninteracting CIM can be calculated from the RE, and then inverted by an adaptation of the iterative bisection algorithm of Ref. 44. Finally, the i-DFT potentials can be obtained by subtraction as in Eq. (5). The map $(v, V) \to (N, I)$ is invertible for all V and the codomain is $|I| \leq \frac{\gamma}{2}N$ for $N \in [0, \mathcal{M}]$ and $|I| \leq \frac{\gamma}{2}(2\mathcal{M} - N)$ for $N \in [\mathcal{M}, 2\mathcal{M}]$. The xc potentials are shown in Fig. 3 for $\mathcal{M} = 3$. Like in the Anderson model the Hxc gate (xc bias) exhibits smeared steps of height $U/2$ (U) but the pattern of their edges is more complex. The equilibrium xc discontinuities of $v_{\mathrm{Hxc}}[N, 0]$ at integer N bifurcate with N-dependent slopes, and at every high-current intersection the slopes of the step edges change.

In the attempt of disentangling the intricate pattern of discontinuity-lines we realized the existence of a duality between intersections in the xc potentials and plateaus in the particle number and current. From the RE of the degenerate CIM a plateau is uniquely identified by a

couple of integers (m,n) with $m,n = 0,\ldots,2\mathcal{M}$; hence the number of plateaus is correctly given by $(2\mathcal{M}+1)^2$. In the (m,n)-plateau with $n \geq m$ the probabilities $P(q)$, $q = m,\ldots,n$ of finding q particles are all identical and given by $P^{-1}(q) \equiv P_{n\geq m}^{-1} = \sum_{j=m}^{n}\binom{2\mathcal{M}}{j}$, whereas all other probabilities vanish. The corresponding particle number and current are therefore

$$N = N_{n\geq m} \equiv P_{n\geq m}\sum_{j=m}^{n} j\binom{2\mathcal{M}}{j}, \tag{12a}$$

$$I = I_{n\geq m} \equiv \frac{\gamma}{2}P_{n\geq m}\sum_{j=m}^{n-1}(2\mathcal{M}-j)\binom{2\mathcal{M}}{j}. \tag{12b}$$

Similarly, for $n \leq m$ one finds $N = N_{n\leq m} = N_{m\geq n}$ and $I = I_{n\leq m} = -I_{m\geq n}$. The intersections in the xc potentials of Fig. 3 occur precisely at the points $(N_{n\geq m}, I_{n\geq m})$ and $(N_{n\leq m}, I_{n\leq m})$. Knowledge of these points allows us to generalize the parametrization in Eqs. (11)

$$v_{\mathrm{Hxc}}^{(\mathcal{M})}[N,I] = \frac{U}{4}\sum_{K=1}^{2\mathcal{M}-1}\sum_{s=\pm}\left[1 + \frac{2}{\pi}\operatorname{atan}\frac{\Delta_K^{(s)}(N,I)}{W}\right] \tag{13a}$$

$$V_{\mathrm{xc}}^{(\mathcal{M})}[N,I] = -U\sum_{K=1}^{2\mathcal{M}-1}\sum_{s=\pm}\frac{s}{\pi}\operatorname{atan}\frac{\Delta_K^{(s)}(N,I)}{W} \tag{13b}$$

where $\Delta_K^{(s)}(N,I)$ is the piece-wise linear function of N and I which vanishes along the step edge passing through $(K,0)$ and having positive $(s = +)$ or negative $(s = -)$ slopes (for examples see dashed lines in top panel of Fig. 3). Here W is the same fitting parameter as in Eq.(11). We verified (not shown) that the self-consistent solution of the KS equations with the xc-potentials of Eqs. (13) are in excellent agreement with the RE results.

Using the analytic parametrization of the xc bias in Eq. (13b) we can calculate the zero-bias conductance from Eq. (8). The result is

$$\frac{G}{G_s} = \frac{1}{1 + \frac{2UG_s}{\gamma\pi W}\sum_{K=1}^{2\mathcal{M}-1}\frac{\frac{1}{2\mathcal{M}-K+1}+\frac{1}{K+1}}{1+(\frac{N-K}{W})^2}}. \tag{14}$$

The correction to G_s is large for integer N's and Eq. (14) can be approximated as $\frac{G}{G_s} \simeq 1/[1 + \frac{2UG_s}{\gamma\pi W}(\frac{1}{2\mathcal{M}-N+1} + \frac{1}{N+1})]$. Thus, the height of the conductance peaks depends on the number of electrons in the junction; the closer we get to half-filling the larger the height is.

Multiple-level CIM and finite bias conductance The potentials in Eq. (13) are not suited to study junctions with nondegenerate levels as the dependence on the local occupations cannot be reduced to a dependence on N only. New interesting aspects arise which are best illustrated in a HOMO-LUMO CIM with energies $\epsilon_i = \epsilon_{H/L} + v$ of degeneracy $\mathcal{M}_{H/L}$. Let $N_{H/L}$ be the particle number on the HOMO/LUMO level, and $v_{\mathrm{Hxc}}[N_H,N_L,I](H/L)$ and $V_{\mathrm{xc}}[N_H,N_L,I]$ be the

HOMO/LUMO Hxc gate and xc bias respectively. For $N_L = 0$ (empty LUMO) we have $v_{\mathrm{Hxc}}(H) = v_{\mathrm{Hxc}}(L)$ (uniform Hxc gate) and the i-DFT potentials are given by Eqs. (13) with $\mathcal{M} = \mathcal{M}_H$. Similarly for $N_H = 2\mathcal{M}_H$ (full HOMO) the Hxc gate is uniform and the i-DFT potentials are again given by Eqs. (13) but with $\mathcal{M} = \mathcal{M}_L$. At zero current $N_H \simeq N$ and $N_L \simeq 0$ or $N_H \simeq 2\mathcal{M}_H$ and $N_L \simeq N - 2\mathcal{M}_H$ are the only physically realizable occupations. Hence, at least for small currents, v_{Hxc} is uniform [45] and can be parametrized by combining the Hxc gate of two CIMs with degeneracy $\mathcal{M} = \mathcal{M}_{H/L}$. This argument remains valid for an arbitrary number of levels; below we therefore show how to construct the i-DFT potentials for the general case.

Let $n = \{n_1\ldots n_{\mathcal{M}}\}$ be the occupations of levels $\{1\ldots\mathcal{M}\}$, $\mathcal{M}_p[n]$ the degeneracy of the p-th largest occupation and $\mathcal{D}[n]$ the number of distinct densities. For instance if $\mathcal{M} = 5$ and $n = \{\frac{1}{3}, \frac{1}{2}, \frac{1}{2}, \frac{1}{3}, \frac{1}{3}\}$ then $\mathcal{M}_1 = 2$, $\mathcal{M}_2 = 3$ and $\mathcal{D} = 2$. We further define $\mathcal{N}_p[n] = 2\sum_{q=1}^{p-1}\mathcal{M}_q[n]$ as the maximum number of particles in the first $(p-1)$ degenerate levels $(\mathcal{N}_1 = 0)$. The degeneracies $\mathcal{M}_p$ are used to construct the following i-DFT potentials

$$v_{\mathrm{Hxc}}[n,I] = \sum_{p=1}^{\mathcal{D}[n]} v_{\mathrm{Hxc}}^{(\mathcal{M}_p[n])}[N - \mathcal{N}_p[n], I]$$
$$+ \frac{U}{4}\sum_{p=1}^{\mathcal{D}[n]-1}\sum_{s=\pm}\left[1 + \frac{2}{\pi}\operatorname{atan}\frac{N + \frac{2s}{\gamma}I - \mathcal{N}_{p+1}[n]}{W}\right], \tag{15a}$$

$$V_{\mathrm{xc}}[n,I] = \sum_{p=1}^{\mathcal{D}[n]} V_{\mathrm{xc}}^{(\mathcal{M}_p[n])}[N - \mathcal{N}_p[n], I]$$
$$- U\sum_{p=1}^{\mathcal{D}[n]-1}\sum_{s=\pm}\frac{s}{\pi}\operatorname{atan}\frac{N + \frac{2s}{\gamma}I - \mathcal{N}_{p+1}[n]}{W}. \tag{15b}$$

where, again, W is defined as before.

The dependence on the local occupations enters exclusively through the $\mathcal{M}_p$. At the joining points $(N = \mathcal{N}_{p+1}[n]$ and $I = 0)$ between two consecutive $v_{\mathrm{Hxc}}^{(\mathcal{M}_p[n])}$ we add a discontinuity with slopes $\pm 2/\gamma$. In fact, the slope of the lines delimiting the domain of the i-DFT potentials of a $\mathcal{M}$-fold degenerate CIM are independent of $\mathcal{M}$, see Figs. 2 and 3. The i-DFT potentials in Eqs. (15) reduce to those in Eqs. (13) for equal occupations $n_i = N/\mathcal{M}$ and to the equilibrium DFT potentials of Ref. 11 for $I = 0$. Furthermore, they can easily be generalized to CIM with local interactions $\frac{1}{2}\sum_{i\sigma\neq j\sigma'}U_{ij}\hat{n}_{i\sigma}\hat{n}_{j\sigma'}$ and level-dependent broadenings $\Gamma_{\alpha,ij} = \delta_{ij}\gamma_i/2$.

To demonstrate the improvement of i-DFT over Landauer+DFT we calculate the finite-bias differential conductance dI/dV of a benzene junction and benchmark the results against the RE. The benzene is described by a six-level CIM with $U = 0.5$ eV and $\varepsilon_i = \varepsilon_i^0 + v$ where $\varepsilon_1^0 = -\varepsilon_6^0 = 5.08$ eV, $\varepsilon_2^0 = \varepsilon_3^0 = -\varepsilon_4^0 = -\varepsilon_5^0 = -2.54$
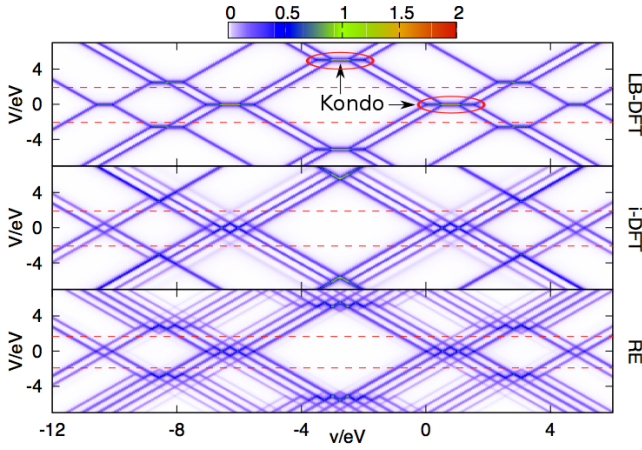
FIG. 4. Differential conductance (in units of the quantum of conductance) calculated from Landauer+DFT (top), i-DFT (middle) and RE (bottom), for a six-level CIM modelling benzene. Dashed red lines delimit the low-bias region where i-DFT and RE agree.

eV. [46] In Fig. 4 we report the dI/dV in the three approaches. Above T_K no Kondo plateau is expected. The Landauer+DFT scheme (top panel) does instead produce Kondo plateaus at zero [16–18] and *nonzero* biases. Furthermore, it misses several dI/dV lines as compared to RE (bottom panel), thus providing a completely erroneous description of CB. The i-DFT scheme (middle panel) correctly suppresses the spurious Landauer+DFT Kondo plateaus, and reproduces the RE trend of the CB peak-heights, see Eq. (14) and discussion below. At small bias, i-DFT captures *all* the dI/dV lines present in the RE approach while at higher bias some lines are missing. This latter fact is not surprising as our model xc potentials is designed to be accurate only at small currents.

In general, the RE approach requires the solution of a linear system of size $4^{\mathcal{M}}$. In contrast, i-DFT requires the solution of $\mathcal{M}$ coupled nonlinear equations. If one aims only at describing the low-bias features correctly, in i-DFT the solution of two coupled equations is sufficient, independent of the size of the system.

Conclusions We propose the i-DFT framework to calculate the steady density and current of interacting junctions at finite bias. i-DFT is based on the invertibility of the map between (n, I) and (v, V) in a finite bias window. Unlike the Landauer+DFT approach, i-DFT naturally leads to xc bias corrections, and in contrast to TD(C)DFT, the i-DFT xc potentials are history-independent. We unveil the complex structure of the i-DFT xc potentials in the CB regime by reverse engineering the occupations and current of a CIM as obtained from the RE. We found that the bifurcations of the xc discontinuity as current starts flowing are pivotal for the correct description of CB. Similarly to the equilibrium xc discontinuity of standard DFT the bifurcations are an

intrinsic property of the i-DFT potentials, and are expected to occur in the **r**-space formulation as well.

We also find an efficient parametrization of the i-DFT potentials for small currents and use it to calculate the finite bias conductance of a model benzene junction. Compared to Landauer+DFT, i-DFT shows a clear improvement, being able to reproduce all the (small bias) dI/dV lines of the RE approach.

[1] G. Cuniberti, G. Fagas, and K. Richter, *Introducing Molecular Electronics* (Springer, Heidelberg, 2005).
[2] J. Cuevas and E. Scheer, *Molecular Electronics: An Introduction to Theory and Experiment* (World Scientific, London, 2010).
[3] J. Taylor, H. Guo, and J. Wang, Phys. Rev. B **63**, 245407 (2001).
[4] M. Brandbyge, J.-L. Mozos, P. Ordejón, J. Taylor, and K. Stokbro, Phys. Rev. B **65**, 165401 (2002).
[5] A. Pecchia and A. D. Carlo, Rep. Prog. Phys. **67**, 1497 (2004).
[6] A. R. Rocha, V. M. García-Suárez, S. Bailey, C. Lambert, J. Ferrer, and S. Sanvito, Phys. Rev. B **73**, 085414 (2006).
[7] A. Arnold, F. Weigend, and F. Evers, J. Chem. Phys. **126**, 174101 (2007).
[8] C. Toher, A. Filippetti, S. Sanvito, and K. Burke, Phys. Rev. Lett. **95**, 146402 (2005).
[9] M. Koentopp, K. Burke, and F. Evers, Phys. Rev. B **73**, 121403 (2006).
[10] S. Kurth, G. Stefanucci, E. Khosravi, C. Verdozzi, and E. K. U. Gross, Phys. Rev. Lett. **104**, 236801 (2010).
[11] S. Kurth and G. Stefanucci, Phys. Rev. Lett. **111**, 030601 (2013).
[12] Z.-F. Liu and K. Burke, Phys. Rev. B **91**, 245158 (2015).
[13] P. Schmitteckert and F. Evers, Phys. Rev. Lett. **100**, 086401 (2008).
[14] H. Mera, K. Kaasbjerg, Y. M. Niquet, and G. Stefanucci, Phys. Rev. B **81**, 035110 (2010).
[15] H. Mera and Y. M. Niquet, Phys. Rev. Lett. **105**, 216408 (2010).
[16] G. Stefanucci and S. Kurth, Phys. Rev. Lett. **107**, 216401 (2011).
[17] J. P. Bergfield, Z.-F. Liu, K. Burke, and C. A. Stafford, Phys. Rev. Lett. **108**, 066801 (2012).
[18] P. Tröster, P. Schmitteckert, and F. Evers, Phys. Rev. B **85**, 115409 (2012).
[19] G. Stefanucci and C.-O. Almbladh, Phys. Rev. B **69**, 195318 (2004).
[20] G. Stefanucci and C.-O. Almbladh, EPL (Europhysics Letters) **67**, 14 (2004).

[21] F. Evers, F. Weigend, and M. Koentopp, Phys. Rev. B **69**, 235411 (2004).

[22] N. Sai, M. Zwolak, G. Vignale, and M. Di Ventra, Phys. Rev. Lett. **94**, 186810 (2005).

[23] E. Runge and E. K. U. Gross, Phys. Rev. Lett. **52**, 997 (1984).

[24] G. Vignale and M. Rasolt, Phys. Rev. Lett. **59**, 2360 (1987).

[25] S. K. Ghosh and A. K. Dhara, Phys. Rev. A **38**, 1149 (1988).

[26] G. Vignale and W. Kohn, Phys. Rev. Lett. **77**, 2037 (1996).

[27] Since an asymmetric bias $V_L \neq -V_R$ between left (L) and right (R) electrodes is equivalent to a symmetric bias $V_L = -V_R = V/2$ and a uniform shift of the nuclear potential $v_n(\mathbf{r})$, we only consider symmetric situations.

[28] G. Stefanucci and R. van Leeuwen, *Nonequilibrium Many-Body Theory of Quantum Systems: A Modern Introduction* (Cambridge University Press, Cambridge, 2013).

[29] D. Bohr, P. Schmitteckert, and P. Wölfle, EPL (Europhysics Letters) **73**, 246 (2006).

[30] N. D. Mermin, Phys. Rev. **137**, A1441 (1965).

[31] J. Riess and W. Münch, Theoret. Chim. Acta **58**, 295 (1981).

[32] X. Gonze, P. Ghosez, and R. W. Godby, Phys. Rev. Lett. **74**, 4035 (1995).

[33] X. Zheng, F. Wang, C. Y. Yam, Y. Mo, and G. Chen, Phys. Rev. B **75**, 195127 (2007).

[34] G. Vignale, Phys. Lett. A **209**, 206 (1995).

[35] V. U. Nazarov, J. M. Pitarke, Y. Takada, G. Vignale, and Y.-C. Chang, Phys. Rev. B **76**, 205103 (2007).

[36] G. Stefanucci, S. Kurth, E. K. U. Gross, and A. Rubio, Theor. Comput. Chem. **17**, 247 (2007).

[37] C. W. J. Beenakker, Phys. Rev. B **44**, 1646 (1991).

[38] Y. Oreg, K. Byczuk, and B. I. Halperin, Phys. Rev. Lett. **85**, 365 (2000).

[39] H. Haug and A.-P. Jauho, *Quantum Kinetics in Transport and Optics of Semiconductors* (Springer, New York, 2008).

[40] K. Walczak, Cent. Eur. J. Phys. **4**, 8 (2006).

[41] We notice that $J_V < 0$ in an infinite bias window even for *arbitrary* noninteracting junctions with frequency-independent matrices Γ_α. It is indeed a matter of simple algrabra to show that $J_V = -2\sum_\alpha a_\alpha t_\alpha$ where $a_\alpha = \int f'(\omega + s_\alpha V/2)\mathrm{Tr}[\mathcal{G}(\omega)\Gamma_\alpha\mathcal{G}^\dagger(\omega)] < 0$ and $t_\alpha = 2\int f'(\omega + s_\alpha V/2)T(\omega) < 0$.

[42] P. Schmitteckert, M. Dzierzawa, and P. Schwab, Phys. Chem. Chem. Phys. **15**, 5477 (2013).

[43] B. Muralidharan, A. W. Ghosh, and S. Datta, Phys. Rev. B **73**, 155410 (2006).

[44] G. Xianlong, A.-H. Chen, I. V. Tokatly, and S. Kurth, Phys. Rev. B **86**, 235139 (2012).

[45] At zero current the uniformity of the Hxc gate can be proved analytically, see Stefanucci, G. and Kurth, S, *Phys. Stat. Sol. B* **2013** *250*, 2378.

[46] The CIM accounts only for the direct Coulomb terms which, however, are sufficient for a qualitative description of the CB. The CIM parameters are taken from the Pariser-Parr-Pople model of benzene, see, e.g., Bursill, R.J., Castleton, C. and Barford, W. *Chem. Phys. Lett.* **1998** *294*, 305.